Final version of the statistical wave model

Vitali Shastun, Oleksiy Agapitov, Vladimir Krasnoselskikh, Michail Balikhin & Simon Walker

Laboratoire de Physique et Chimie de l'Environnement
SSL, University of California at Berkeley
Departemant of Automatic Control, University of Sheffield

Work package specific tasks

Task 4.1 Collection of data and the development of software for automatic identification of Chorus, hiss and equatorial magnetosonic emissions
Task 4.2 Preparation of data sets for Error Reduction Ratio analysis Month 3-6 (LPC2E, USD)
Task 4.3 Error reduction analysis. Month 7-10 (USD)
Task 4.4 Development of the Statistical Wave Models and corresponding tensors of diffusion coefficients. Month 11-24 (LPC2E, SIST)

Spacecraft missions

Mission	Dates	Instrument	Coverage		Spectral
			λ	L	coverage
DE-1	1981-1984	PWI SFR	$< 20°$	2-8	< 410 kHz
POLAR	1996-1997	PWI SFR	$< 90°$	> 2	< 800 kHz
CRRES	1990-1991	PWE SFR	$< 15°$	2-8	< 400 kHz
		Control parameters model:			
THEMIS 3 s/c	2008-2015	SCM FBK	$< 20°$	3-8	< 4 kHz
Cluster 4s/c	2001-2015	STAFF	$< 45°$	> 3	< 4 kHz
		λ-K_P model:			
RBSP 2 s/c	2012-2015	EMFISIS	$< 20°$	2-6	< 30 kHz

Table: The set of spacecraft missions used to construct the database

Cluster coverage

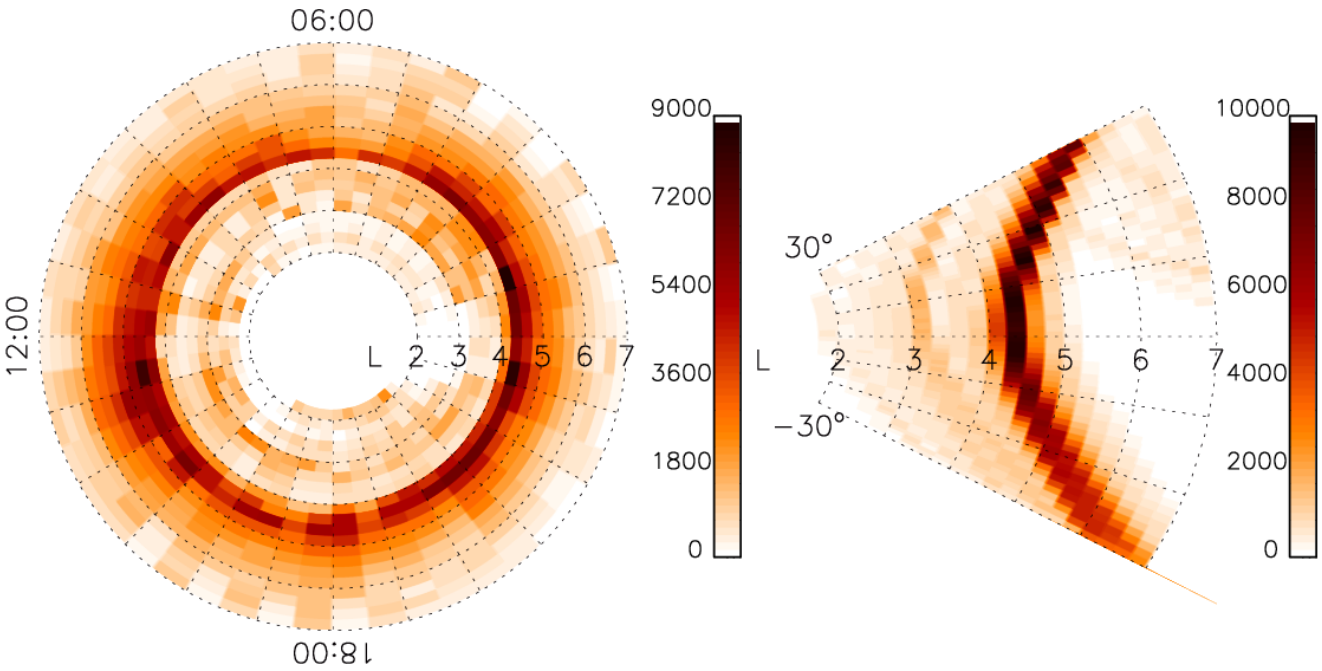

Figure: The orbital coverage of Cluster spacecraft during 2001-2010 in dependence on L-shell/MLT (left panel) and L-shell/λ (right panel).

Themis coverage

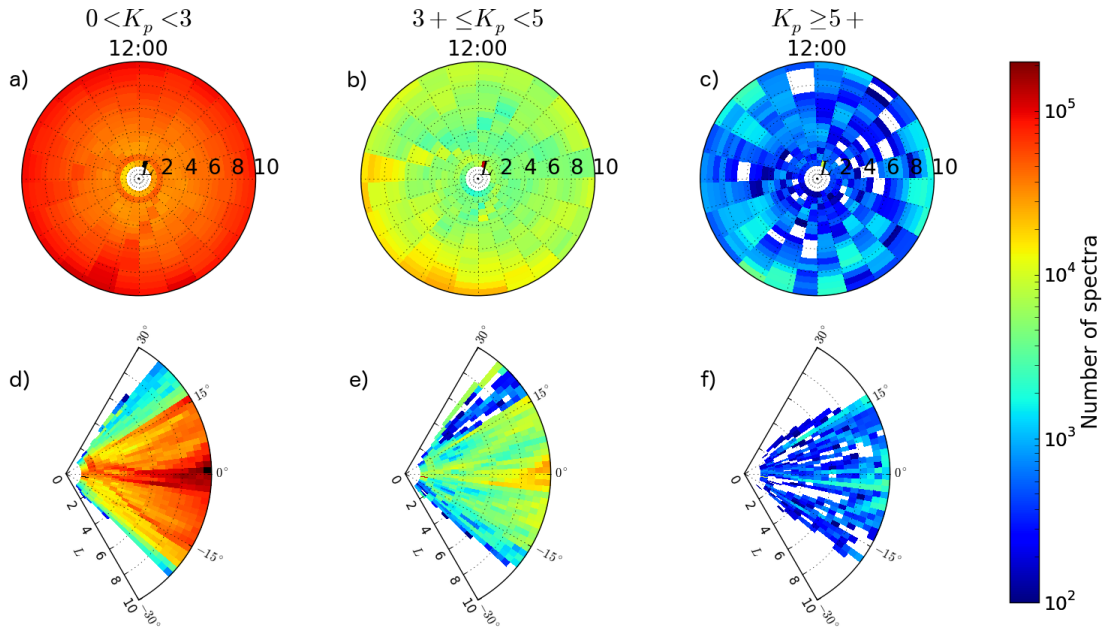

Figure: The orbital coverage of THA spacecraft during 2008-2014 in dependence on L-shell/MLT (top panels) and L-shell/λ (bottom panels) frames for periods of low ($K_p < 3$) (a and d), intermediate ($3 \leq K_p < 5$) (b and e) and high geomagnetic activity ($K_p > 5$) (c and f).

Solar wind data and geomagnetic activity indices

Table: List of control parameters used to develop wave activity models.

	Abbreviation	Description
1.	V_{sw}	1-hour velocity of solar wind $[km/s]$.
2.	N	1-hour concentration of solar wind $[cm^{-3}]$.
3.	P	Flow pressure of solar wind $[nPa]$.
4.	AE	1-hour AE index [nT].
5.	Dst	1-hour Dst index [nT].
6.	Bt	IMF factor [nT].

Model of two control parameters

Amplitude of wave magnetic field B_w:

$$B_w = \sqrt{\sum_{i=1}^{n} a_i A_i^2} \qquad a_i = \begin{cases} 1, & \text{if } 0.1 f_{ce} < f_i < 0.5 f_{ce} \\ 0, & \text{otherwise} \end{cases}$$

A_i - amplitude in i-th channel, f_{ce} - electron cyclotron frequency, f_i - central frequency of i-th channel.

Analytical form of RMS wave magnetic field amplitudes $\langle B_w \rangle$:

$$\log_{10} \langle B_w \rangle = \sum_{i=0}^{3} \sum_{j=0}^{3} a_{ij} cp_1^i cp_2^j$$

$cp1$ and $cp2$ - control parameters, aij - coefficients of the model.

LBC wave models

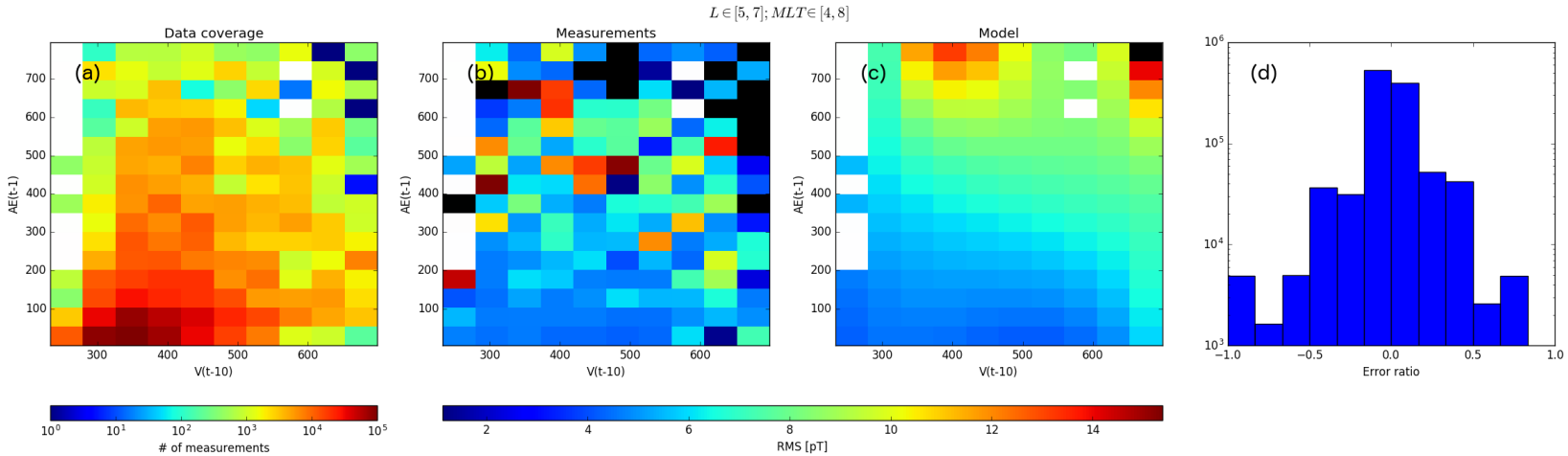

Figure: (a) Data coverage of the Cluster STAFF-SA and THEMIS FBK measurements in the LBC frequency range ($0.1\omega_{ce} < \omega < 0.5\omega_{ce}$) as a number of spectra captured in V_{sw}-AE domain for $5 < L < 7$ and $04:00 - 08:00$ MLT. (b) RMS of LBC magnetic field amplitude in V_{sw}-AE domain measured by Cluster and THEMIS probes. (c) RMS values obtained from the analytical model developped using the measurements. (d) Distribution of discrepancies between analytical model and actual measurements.

Hiss wave models

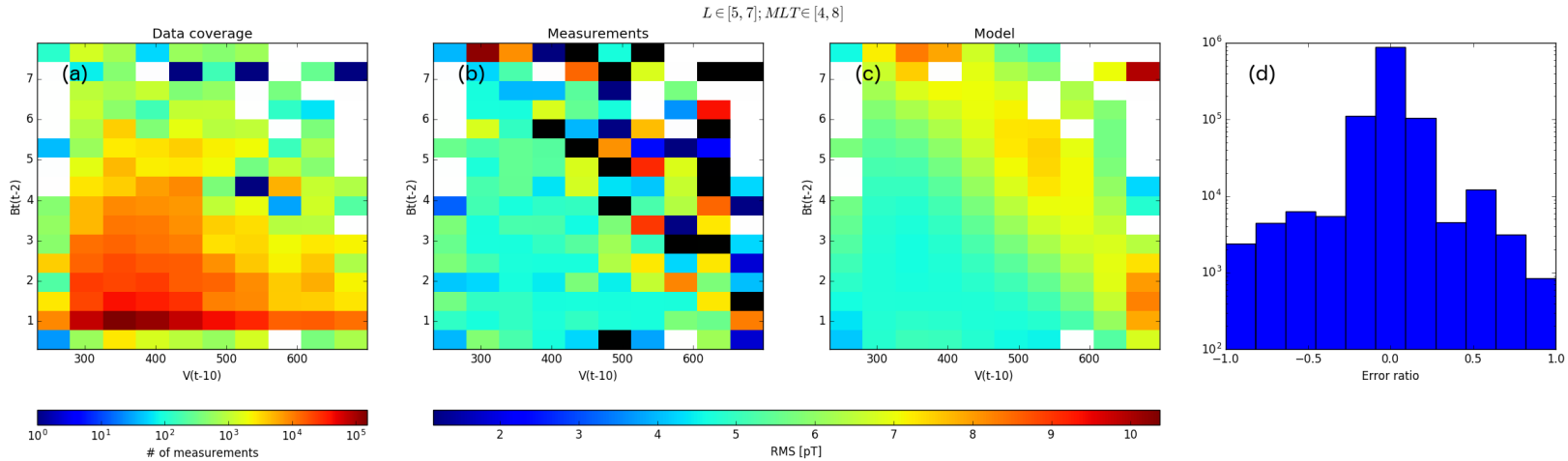

Figure: Data coverage, measured and analytical values of RMS of magnetic field amplitudes in V_{sw}-Bt domain for region $5 < L < 7$ and 04:00-08:00 MLT in same format as Figure 3.

EMW wave models

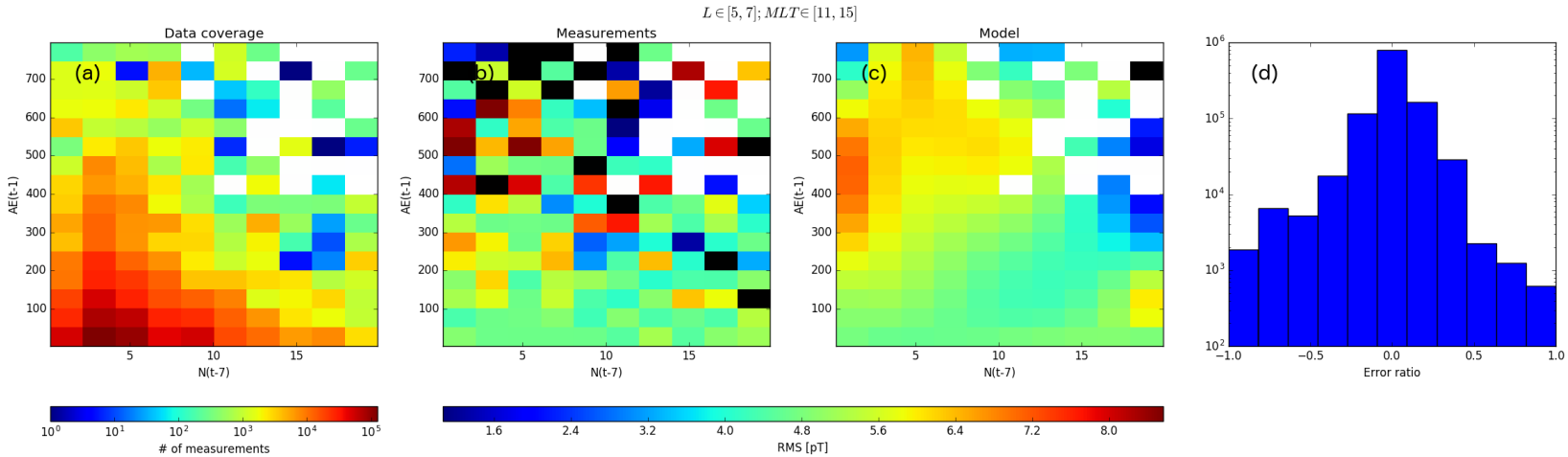

Figure: Data coverage, measured and analytical values of RMS of magnetic field amplitudes in N-AE domain for region $5 < L < 7$ and 11:00-15:00 MLT in same format as Figure 3.

RMS of wave amplitudes B_w and obliquity parameter Q as a function of K_p and λ

$$\log_{10} B_w(L, \lambda, K_P) = \sum_{i=0}^{3} \sum_{j=0}^{3} a_{ij} (\lambda[^\circ]/10)^i L^j \sum_{k=0}^{3} b_k K_P^k,$$

$$Q(L, \lambda, K_P) = \sum_{i=0}^{3} \sum_{j=0}^{3} a_{ij} (\lambda[^\circ]/10)^i L^j \sum_{k=0}^{3} b_k K_P^k,$$

$$Q = \sum_{\theta=\theta_{Gen}}^{\theta=\theta_{res}} N(\theta)/N_{total}$$

where θ_{Gen}, θ_{res} - Gendrin and resonance cone angles, a_{ij}, b_k - coefficients of the model.

Characteristics of LBC in λ-K_P domain

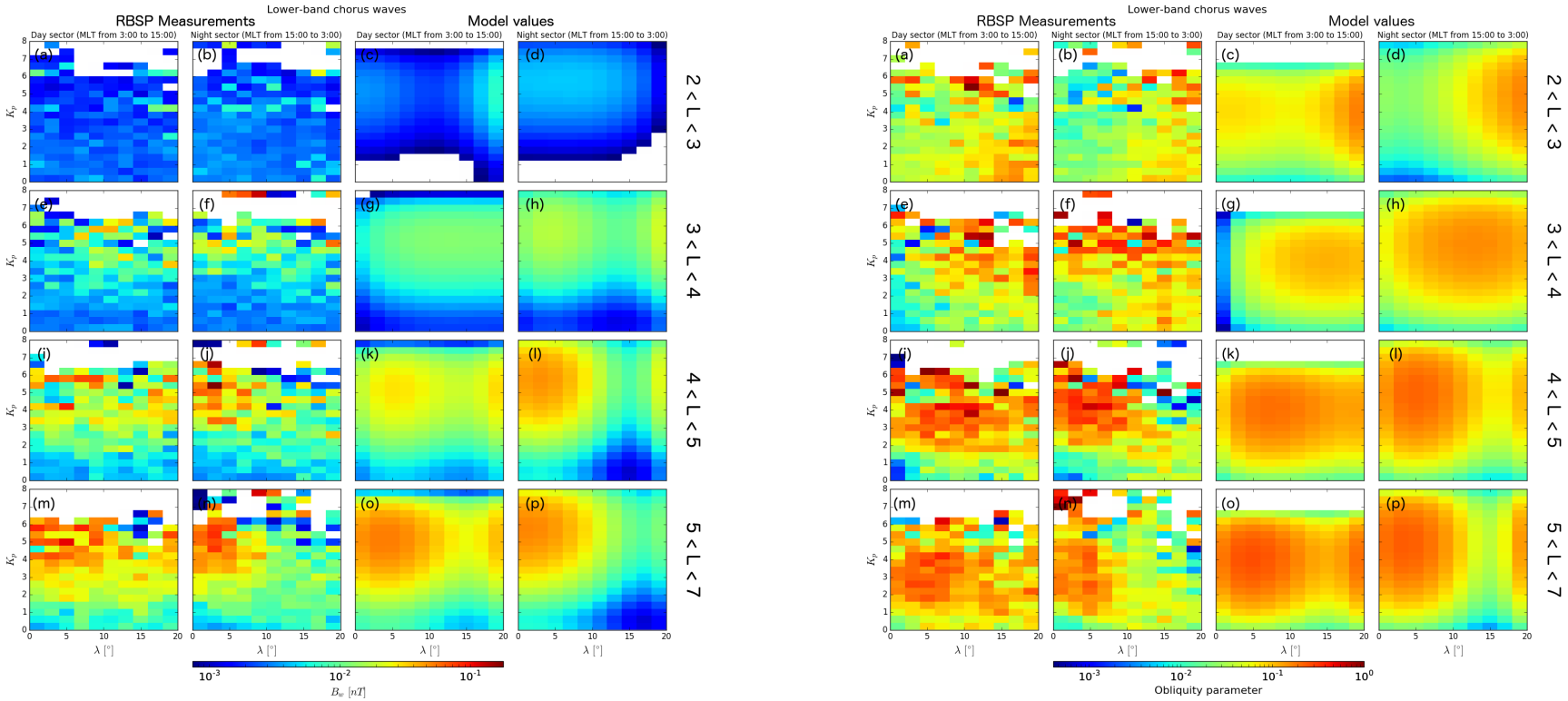

Distributions of the $\langle B_w \rangle$ (left) and Q (right) of LBC waves in λ-K_P domain as registered by RBSP probes during 2012-2015.

Characteristics of hiss in λ-K_P domain

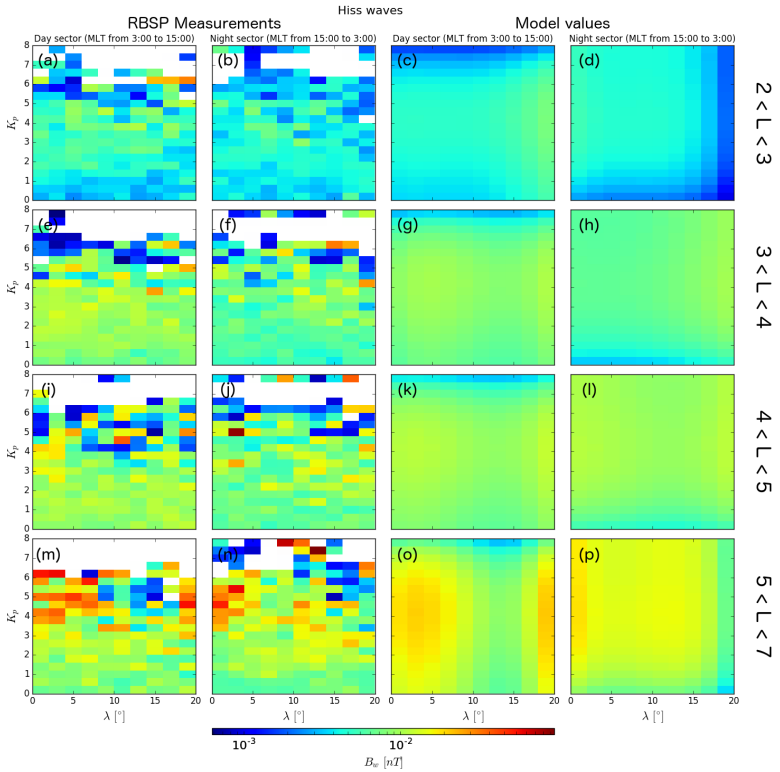

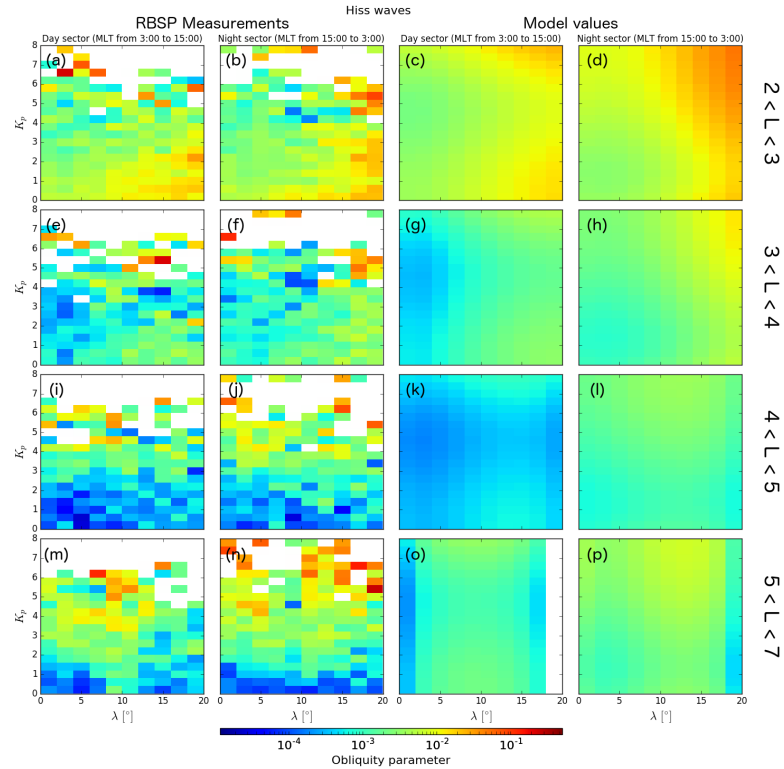

Distributions of the $\langle B_w \rangle$ (left) and Q (right) of hiss waves in λ-K_P domain as registered by RBSP probes during 2012-2015.

Conclusions

- Data base of whistler waves was collected in a vicinity of the geomagnetic equator (chorus generation region).
- It is found that vast amount of data is available to be analysed, comprehensively covering all magnetic local times (MLT) and L-shell in the range $4 < L < 7$ for a wide range of geomagnetic activity $K_P \in [0, 6]$.
- The new statistical wave models are built with respect to the lags of the geomagnetic indices and solar wind parameters identified by ERR and therefore account previous evolution of the magnetosphere's state.
- The polynomial wave models provide the needed information as a function of geomagnetic activity.